Springer

KSME

Journal of Mechanical Science and Technology 31 (9) (2017) 4419~4423
www.springerlink.com/content/1738-494x(Print)/1976-3824(Online)
DOI 10.1007/s12206-017-0842-5

Experimental investigation of in-process mitigation of welding distortion for stainless steel plate using air-atomized mist cooling †

Sung-Min Joo[1], Young-Gon Kim[2] and Se-Min Jeong[3,*]

[1]*Department of Welding & Joining Science Engineering, Chosun University, Gwangju 61452, Korea*
[2]*Green Manufacturing Process R&D Group, KITECH, Gwangju 500-460, Korea*
[3]*Department of Naval Architecture and Ocean Engineering, Chosun University, Gwangju 61452, Korea*

(Manuscript Received March 23, 2017; Revised May 3, 2017; Accepted May 14, 2017)

Abstract

In this study, welding-induced out-of-plane distortion of stainless steel sheets is examined in the case of applying air-atomized mist jet on the rear side of the weld pool. An internally mixed type air atomizing spray nozzle is attached to the welding torch and both are moved at the same speed and direction onto the welding centerline. The test specimens are 2 mm thick grade 304 stainless steel plates. Bead-on-plate welds are made on the plates using a DC Gas tungsten arc welding (GTAW) process. The measured welding distortion and residual stresses are compared with those of a conventional GTAW welding process. The experimental results show that the welds performed with a trailing heat sink using air-atomized mist have almost zero out-of-plane distortion. In addition, a slight welding residual stress reduction is achieved.

Keywords: Heat sink welding; Mist nozzle; Welding deformation; Welding residual stress

1. Introduction

Welding is an economical manufacturing process to assemble structures in many industrial fields. However, during the welding process, locally concentrated heat is applied to the welded joint. This imposes local steep temperature gradients that produce high gradients in thermal expansion. The expanding material is thereby restrained by the surrounding cooler base metal causing plastic deformation. As the weld zone is cooled down to room temperature, welding-induced distortion and residual stresses are produced.

Usually, the welding residual stress level of the weld zone is close to the yield stress of the welded material. These high stresses are responsible for stress corrosion cracking and fatigue crack growth in the weld zone, which shorten the service life of the welded structure.

Welding-induced distortion leads to precision problems and fixing the dimensional tolerances incurs additional costs after the welding process [1]. Mitigation of welding residual stress and welding deformation requires an additional process to mechanically or thermally alleviate these problems after the completion of welding in most cases [2, 3].

However, the application of in-process control techniques such as Heat sink welding (HSW) and Low-stress no distortion (LSND) welding would be more economical.

The existing parameters such as electric current, voltage, and welding speed are required in addition to the new parameters, including the distance between the heat sink and welding arc, strength of heat sink, and size of heat sink.

The LSND technique was studied by Guan et al. [4-6]. They reported that during Gas tungsten arc welding (GTAW) of 1 mm thick mild steel and stainless steel, trailing welding, where a heat sink trails a welding arc, is effective in preventing buckling.

To control welding-induced stresses and distortion by using the LSND process, liquid CO_2 and liquid nitrogen are applied as a heat sink medium; however, they are cost-intensive.

On a numerically simulated HSW using a semicylindrical pipe where water flows at the time of multipass GTAW welding of 10 mm thick Monel 400 alloy plates, Yegaie et al. [7] discovered that there was a reduction in residual stress. In the numerical simulation of HSW for 316L stainless steel using the same method as that of Yegaie et al., Jiang et al. [8] also found a 20 % reduction in the welding residual stress.

In the present study, the rear side of the weld is cooled by using water that is inexpensive and easy to handle.

The water is sprayed by a commercial mist nozzle, which is applied in various industries [9-11]. With the fabricated mist cooling system, HSW is carried out and the variations of out-

*Corresponding author. Tel.: +82 62 230 7218, Fax.: +82 62 230 7135
E-mail address: smjeong@chosun.ac.kr
† Recommended by Associate Editor Young Whan Park

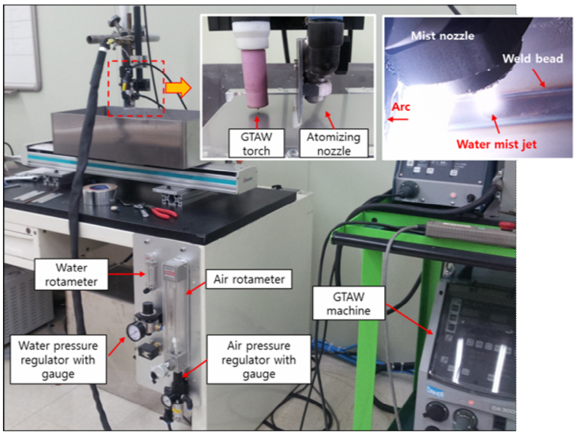

Fig. 1. Photograph of experimental apparatus with mist cooling nozzle.

of-plane distortion are observed in comparison with the conventional welding process.

2. Experimental setup and procedure

The type of welding used in this experiment is GTAW without filler wire. A special setup is added to obtain the desired experimental results. The setup consists of a GTAW torch followed by an atomizing nozzle at a short distance (standoff distance), as shown in Fig. 1.

The stream of atomized water is sprayed along the weld area through a nozzle trailing the welding arc. The mist nozzle is an internal mixing type twin-fluid atomizer, which produces a narrow and full cone round spray pattern. Compressed air and water are sprayed through this mist nozzle and the flow rate is measured by a rotameter.

Autogenous Bead-on-plate (BOP) welds are performed at the center of the specimen except for 30 mm at both ends. The materials used in the experiment are 304 stainless steel with dimensions of 100 × 200 × 2 mm and 150 × 300 × 2 mm. Using these specimens, both conventional GTAW and HSW are carried out to check the feasibility of using mist cooling instead of liquid CO_2 or liquid nitrogen for minimizing out-of-plane distortion.

To prevent intrusion of the atomized water to the arc pool side and maintain arc stability, heat-resistant silicone membrane and ceramic wool are installed between the arc torch and mist nozzle.

All the specimens are not clamped and hence, distortion in out-of-plane direction is not restrained during the welding and cooling processes. The welding current and welding speed are fixed at 100 A and 0.6 m/min, respectively. The conditions for minimizing out-of-plane distortion were determined by varying the standoff distance and flow rate of the mist nozzle.

The out-of-plane distortion, temperature history, and distribution of residual stress are all measured experimentally for comparison between the conventional welding and HSW.

The out-of-plane distortion was measured by using an LVDT (Linear variable differential transformer, TCL-100A)

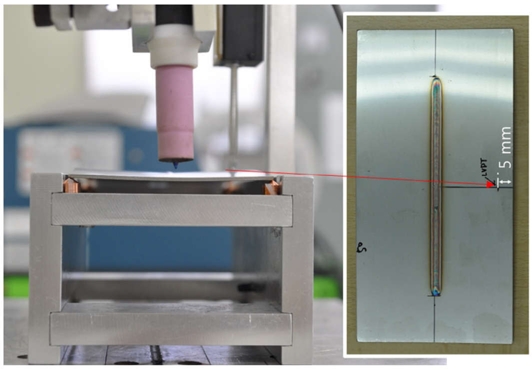

Fig. 2. Location of out-of-plane deformation measurement.

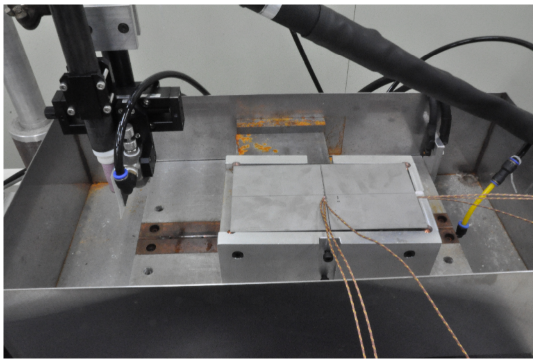

Fig. 3. Measuring points for thermal history.

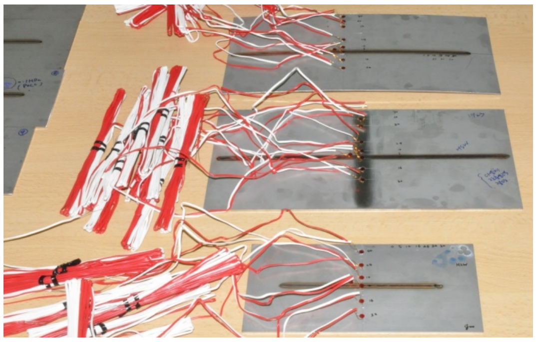

Fig. 4. Photograph of specimens with attached strain gauges for measuring welding residual stresses.

and data logger (TDS303) at a distance of 5 mm from the center of the specimen length in the width direction. The measurement position is shown in Fig. 2.

To measure the thermal histories, a series of K-type thermocouples are spot welded on the specimens as shown in Fig. 3.

The residual stresses in the as-welded specimens for comparison between conventional welding and HSW are measured with sectioning method using strain gauges. The strain gauges of type FCA-1 (gauge length 1 mm, 0°/90° 2-element rosette stacked, 120 Ω) are used for residual stress measurements. The strain gauges are attached at 0, 5, 10, 16, 24, 32 and 40 mm from the weld bead centerline as shown in Fig. 4. The measurements are taken from the top surfaces of each specimen tested. After taking the initial readings, the strain

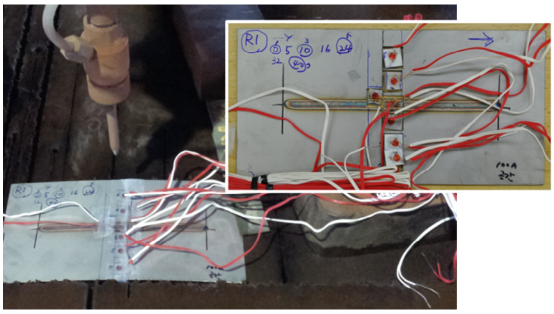

Fig. 5. Water jet cutting of strain gauges attached to welded specimens.

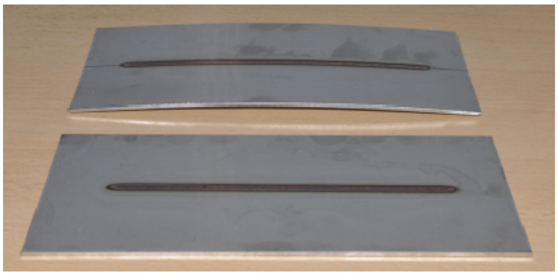

Fig. 6. As-welded specimens of conventional welding (upper) and heat sink welding (lower).

gauges are cut off from the specimens by water jet for stress relaxation as shown in Fig. 5.

3. Results and discussion

3.1 Out-of-plane distortion measurement

The out-of-plane distortion in the conventional welding is convex shape as shown in Fig. 6, and 4.5 mm out-of-plane distortion occurs at the LVDT measuring point. On the other hand, completely distortion-free results are obtained in both 100 × 200 × 2 mm and 150 × 300 × 2 mm specimens by applying HSW using mist cooling as shown in Fig. 6.

The mist sprayed onto the specimen surface evaporated immediately after passing through the hot weld bead.

In the case of 25 mm standoff distance, the welding distortion was minimized when the flow rates of compressed air and water were 22-24 L/min at 0.8-0.1 MPa and 80-100 mL/min at 0.08-0.09 MPa, respectively. In this optimum condition, no out-of-plane distortion was observed as shown in Fig. 6.

However, when the standoff distance increases, or when the amount of water and air sprayed is changed from the optimum condition, out-of-plane deformation occurs. For example, Fig. 7 shows the convex and concave deformed shapes at a standoff distance of 30 mm when the mist injection amount is large and when the mist amount is small, respectively.

Throughout the experiment, it is confirmed that the out-of-plane distortion decreases with the decrease in the spacing between the welding arc and the cooling heat sink. HSW is ineffective in reducing distortion when the standoff distance is greater than 50 mm.

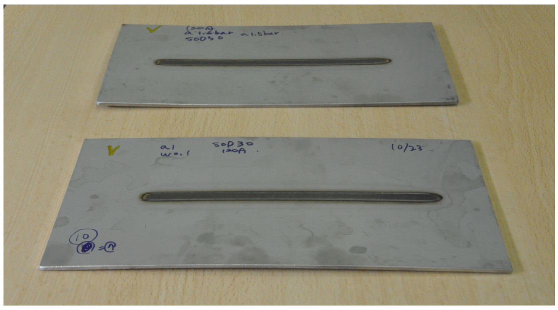

Fig. 7. Concave (upper) and convex deformed shapes (lower) of heat sink welded specimens.

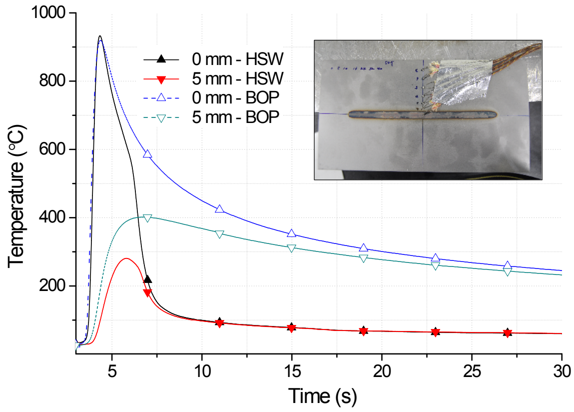

Fig. 8. Thermal history comparison between conventional welding (dotted lines) and heat sink welding (solid lines).

3.2 Thermal measurement

The temperature history for conventional welding and HSW are comparatively measured.

The K-type thermocouples are attached at the bottom side of the specimens on the weld centerline. The temperature histories are measured from the weld centerline as shown in Fig. 8. The heat sink weld shows a steep decrease in temperature as time passes, whereas a more gradual decrease in temperature is observed for conventional welds.

For HSW, it can be observed that the temperature gradient during cooling varies from approximately 6.2 s and the temperature drops more rapidly. It is thought that the mist droplets reach the surface of the weld after 6.2 s under this experimental condition; thus, the welded surface is wet and therefore, the cooling rate is higher than that before 6.2 s. The droplets ejected from the mist nozzle evaporate in the high-temperature atmosphere of the welded zone and cannot reach the surface of the high-temperature welded part due to the evaporation pressure; hence, the cooling rate is lower than that after the wetting temperature. This variation in cooling gradient is similar to that observed by Lee et al. [12] in the case of mist cooling of a high-temperature cylindrical surface. As a result, the temperature is over 400 °C for conventional welding, whereas for HSW, the temperature is rapidly cooled to less than 100 °C after approximately 10 s. These changes affect the strain and

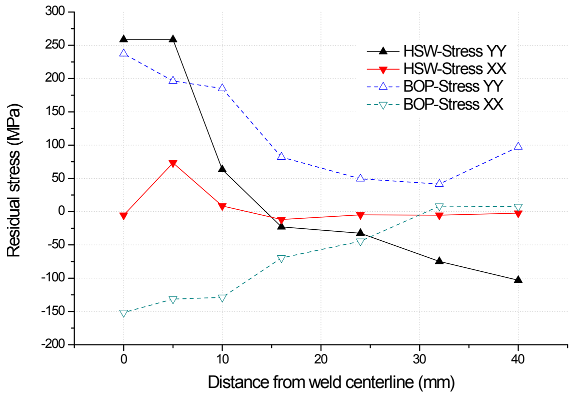

Fig. 9. Measured residual stress distributions for conventional welding and heat sink welding on the top surface of the welded specimens (100 × 200 × 2 mm).

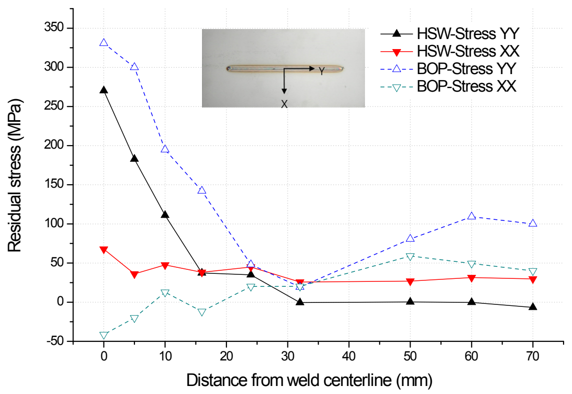

Fig. 10. Measured residual stress distributions for conventional welding and heat sink welding on the top surface of the welded specimens (150 × 300 × 2 mm).

deformation of the welded specimens, and the internal mechanical states are investigated through residual stress measurements.

3.3 Residual stress measurements

A comparison of the welding residual stress distribution between conventional welding (dotted lines) and HSW (solid lines) are shown in Figs. 9 and 10. In the caption of the graphs, XX refers to the transverse residual stress component and YY refers to the longitudinal residual stress component.

Figs. 9 and 10 are the results of the 100 × 200 × 2 mm and 150 × 300 × 2 mm, respectively. The residual stress distribution due to the difference in thermal history between conventional welding and HSW is also very different. In the case of HSW, the variation of the transverse residual stress component is small, and for the longitudinal residual stress component, the amount of the portion where the tensile stress is generated is small. However, there is no significant difference in the maximum magnitude of longitudinal residual stress components occurring near the weld bead.

4. Conclusions

Successful results of experiments on in-process welding distortion control were obtained by applying HSW using mist cooling. In the future, we will test whether mist cooling is effective in reducing out-of-plane distortion even in multipass full penetration welding using a weld filler.

The major findings are summarized as follows:

(1) A significant in-process reduction of weld induced out-of-plane distortion of 2 mm thick stainless steel specimens can be achieved by mist cooling using water as the cooling medium.

(2) The heat sink placed behind the heat source should be as small and as close to the weld pool as possible to obtain the highest out-of-plane distortion mitigation effect. In this experiment, the cooling effect by mist was negligible when the standoff distance was more than 50 mm.

(3) Compared with conventional welding, no significant differences are observed in the maximum values of welding residual stress in the case of mist cooling.

Acknowledgment

This study was supported by a research fund from Chosun University, 2015.

References

[1] J. Wang, H. Zhao, J. Zou, H. Zhou, Z. Wu and S. Du, Welding distortion prediction with elastic FE analysis and mitigation practice in fabrication of cantilever beam component of jack-up drilling rig, *Ocean Engineering,* 130 (2017) 25-39.

[2] F. Tölle, A. Gumenyuk, A. Backhaus, S. Olschok, M. Rethmeier and U. Reisgen, Welding residual stress reduction by scanning of a defocused beam, *Journal of Materials Processing Technology,* 212 (1) (2012) 19-26.

[3] H. Zhang, G. Zhang, C. Cai, H. Gao and L. Wu, Fundamental studies on in-process controlling angular distortion in asymmetrical double-sided double arc welding, *Journal of Materials Processing Technology,* 205 (1-3) (2008) 214-223.

[4] Q. Guan, C. X. Zhang and D. L. Guo, Dynamic control of welding distortion by moving spot heat sink, *Welding in the World,* 33 (4) (1994) 308-312.

[5] J. Li, Q. Guan, Y. Shi, D. Guo, Y. Du and Y. Sun, Studies on characteristics of temperature field during GTAW with a trailing heat sink for titanium sheet, *Journal of Materials Processing Technology,* 147 (3) (2004) 328-335.

[6] J. Li, Q. Guan, Y. W. Shi and D. L. Guo, Stress and distortion mitigation technique for welding titanium alloy thin sheet, *Science and Technology of Welding and Joining,* 9 (5) (2004) 451-458.

[7] Y. S. Yegaie, A. Kermanpur and M. Shamanian, Numerical simulation and experimental investigation of temperature and residual stresses in GTAW with a heat sink process of Monel 400 plates, *Journal of Materials Processing Technology,* 210 (13) (2010) 1690-1701.

[8] W. Jiang, Y. Zhang and W. Woo, Using heat sink technology to decrease residual stress in 316L stainless steel welding joint: Finite element simulation, *International Journal of Pressure Vessels and Piping,* 92 (2012) 56-62.
[9] M. Aamir, L. Qiang, W. Hong, Z. Xun, J. Wang and M. Sajid, Transient heat transfer performance of stainless steel structured surfaces combined with air-water spray evaporative cooling at high temperature scenarios, *Applied Thermal Engineering,* 115 (2017) 418-434.
[10] D. Babic, D. B. Murray and A. A. Torrance, Mist jet cooling of grinding processes, *International Journal of Machine Tools and Manufacture,* 45 (10) (2005) 1171-1177.
[11] C. Huang and Y. Ye, Development of a water-mist cooling system: A 12,500 Kcal/h air-cooled chiller, *Energy Reports,* 1 (2015) 123-128.
[12] S. Lee, J. Park, P. Lee and M. Kim, Mist cooling of high-temperature cylinder surface, *Transactions of the Korean Society of Mechanical Engineers - B,* 26 (3) (2002) 448-457.
[13] D. Lee and S. Shin, Nonlinear pushover analysis of concrete column reinforced by multi-layered, high strength steel UL700 plates, *Engineering Structures,* 90 (2015) 1-14.
[14] D. Lee and S. Shin, Specimen test of large-heat-input fusion welding method for use of SM570TMCP, *Advances in Materials Science and Engineering,* 2015 (2015) 13.
[15] Y. G. Kim, J. S. Kim and I. J. Kim, Effect of process parameters on optimum welding condition of DP590 steel by friction stir welding, *Journal of Mechanical Science and Technology,* 28 (12) (2014) 5143-5148.

Sung-Min Joo is currently an Assistant Professor at the Department of Welding & Joining Science Engineering, Chosun University. He received his Ph.D. in Naval Architecture and Ocean Engineering from Chosun University in 2005. His research interests include computational weld mechanics and advanced welding processes.

Se-Min Jeong is currently an Assistant Professor at the Department of Naval Architecture & Ocean Engineering, Chosun University. He received his Ph.D. in Environmental & Ocean Engineering in 2007 from the University of Tokyo. His research interests are focused on computational physics particularly on thermal and fluid systems.

Young-Gon Kim is currently a Principal Researcher in the Department of Green Manufacturing Process Technology Center of KITECH. He received his M.S. and Ph.D. degrees from Osaka University. His research interests include friction stir welding along with fusion welding process for automotive.